

## Bonding to Titanium

Richard F. W. Bader\* and Chérif F. Matta

Department of Chemistry, McMaster University, Hamilton, Ontario L8S 4M1, Canada

Received February 8, 2001

The recent synthesis of a crystalline compound containing Ti bonded to cyclopentadienyl and a substituted dienylyl fragment prompted the question of whether Ti–C contacts that were found to be shorter than other such bonded contacts in the same molecule should be considered as short nonbonded contacts or “nonclassical metal-to-saturated-carbon atom interactions”, fitting the description of agostic interactions. This question has a unique answer within the framework of the quantum theory of atoms in molecules (QTAIM). QTAIM uses the measurable electron density to assign a molecular structure and the physics of an open system to determine the nature of the bonded interactions. All of the classical bonding descriptors, when recast in terms of the topologies of the electron density and the pair density, are faithfully recovered when QTAIM is applied to the hydrocarbon framework of the Ti complex, thereby justifying its application to the analysis of the Ti–C interactions. No bond paths are found to link the Ti to the carbons exhibiting the “short contacts”, and the topology of the density gives no indication of an incipient change in structure that would result in their formation.

### Assigning a Bonded Structure

At the Pacificchem 2000 meeting in Honolulu, a session on “The boundary between long bonds and short nonbonds” considered whether a “nonbonded” contact found between a metal atom and a saturated carbon atom that is shorter than bonded carbon–metal separations in the same transition metal molecule should be described as a bonded interaction.<sup>1</sup> If indeed bonded, the interaction would qualify as the first experimental example of an “agostic” bond between a transition metal atom and a saturated carbon, a name previously applied only to metal–hydrogen interactions.<sup>2</sup> This paper presents arguments against such a finding in this molecule on the basis of the quantum theory of atoms in molecules (QTAIM).<sup>3</sup> This paper illustrates how theory enables one to assign a molecular structure to any system for which the electron density is known from either experiment or a theoretical calculation.

A structure is defined by the network of bond paths, a bond path being the unique line of maximum electron density that links the nuclei of neighboring atoms in an equilibrium geometry. Every bond path is mirrored by a “virial path”, a line along which the potential energy density is maximally stabilizing.<sup>4</sup> The presence of a bond path provides a universal indicator of bonding between the atoms that it links, one that is applicable to all types of atomic interactions.<sup>5</sup> In particular, the presence of a bond path linking a titanium atom to a methyl hydrogen in an agostic interaction has been demonstrated in both experimental and theoretical charge distributions.<sup>6,7</sup> The

network of bond paths has been shown to recover the structures familiar to chemists and assigned on the basis of the Lewis electron pair model applied to molecules composed of main group atoms. The Lewis model is, however, not of universal applicability. In particular, it cannot be used to predict whether or not a short nonbonded interaction is indicative of the presence of a bond. It is unable, for example, to account for the bonding found in crystals composed of neutral closed-shell molecules that results from so-called nonbonded interactions, interactions that are readily identified in terms of bond paths. This is exemplified by the bond paths present in both the experimental and theoretical charge distributions of solid chlorine that account for the short—relative to the sum of the van der Waals radii—directed intermolecular interactions responsible for the layered structure exhibited by this crystal, a structure not anticipated when the nonbonded interactions are described using a nondirectional van der Waals potential.<sup>8</sup>

The Lewis model provides the basis for the localized bonded and nonbonded electron pairs assumed in the VSEPR model of molecular geometry,<sup>9</sup> a model that can fail in its application to transition metal molecules, which indicates that the Lewis model can also fail for such molecules. Thus, to account for the bonding in a transition metal molecule and, in particular, to decide on the possible presence of an agostic interaction, it is necessary to understand the limitations of the Lewis model by appealing to the underlying physics.

### Lewis Model and Spatial Pairing of Electrons

The spatial localization of an electron pair to a given atom and its delocalization over a pair of atoms are the physical embodiments of the Lewis concepts of a nonbonded and bonded pair, respectively. The pairing of electrons is a consequence of the Pauli exclusion principle, and the spatial localization of the pairing is determined by the corresponding property of the

- (1) Tomaszewski, R.; Hyla-Kryspin, I.; Mayne, C. L.; Arif, A. M.; Gleiter, R.; Ernst, R. D. *J. Am. Chem. Soc.* **1998**, *120*, 2959.
- (2) Brookhart, M.; Green, M. L. H. *J. Organomet. Chem.* **1983**, 395.
- (3) Bader, R. F. W. *Atoms in Molecules: a Quantum Theory*; Oxford University Press: Oxford, 1990.
- (4) Keith, T. A.; Bader, R. F. W.; Aray, Y. *Int. J. Quantum Chem.* **1996**, *57*, 183.
- (5) Bader, R. F. W. *J. Phys. Chem. A* **1998**, *102*, 7314.
- (6) Popelier, P. L. A.; Logothetis, G. *J. Organomet. Chem.* **1998**, 555, 101.
- (7) Scherer, W.; Hieringer, W.; Spiegler, M.; Sirsch, P.; McGrady, G. S.; Downs, A. J.; Haaland, A.; Pedersen, B. *Chem. Commun.* **1998**, 2471.

- (8) Tsirelson, V.; Zou, P. F.; Bader, R. F. W. *Acta Crystallogr., Sect. A* **1995**, *51*, 143.
- (9) Gillespie, R. J.; Hargittai, I. *The VSEPR Model of Molecular Geometry*; Allyn and Bacon: Boston, 1991.

density of the Fermi hole.<sup>10</sup> The Fermi hole, the physical manifestation of the exclusion principle, has a simple physical interpretation: it provides a description of how the density of an electron of a given spin, called the reference electron, is spread outward from any given point into the space of another same-spin electron, thereby excluding the presence of an identical amount of same-spin density.<sup>10,11</sup> It is a negative quantity, as it decreases the amount of same-spin density throughout space by one electronic charge. If the density of the Fermi hole is maximally localized in the vicinity of the reference point, then all other same-spin electrons are excluded from this vicinity and the reference electron is localized. For a closed-shell molecule, the result is a localized  $\alpha,\beta$  pair. Correspondingly, the electron can go wherever its Fermi hole goes, and if the Fermi hole of an electron, when referenced to a given atom, is delocalized into the basin of a second atom, then the electron is shared between them.<sup>10</sup>

The total density removed by the Fermi hole for one  $\alpha$  electron corresponds to the removal of a single electronic charge, and when weighted by the  $\alpha$ -spin density (the *Fermi correlation* for the  $\alpha$  electrons), it corresponds to the removal of the charge of all the  $\alpha$  electrons,  $N_\alpha$  in number. A corresponding result is obtained for the  $\beta$  electrons, and thus the Fermi correlation for both spins accounts for the spatial behavior of all  $N$  electrons in a quantitative manner.

The above ideas, when used in conjunction with the quantum definition of an atom in a molecule, enable one to determine the extent to which electrons are localized to a given atom and delocalized or shared with other atoms.<sup>10,12</sup> The Fermi correlation contained within a single atomic basin and denoted by  $F(A,A)$  is a measure of the extent to which the  $N(A)$  electrons of atom  $A$  are localized within its basin. Its limiting value is  $-N(A)$ , corresponding to complete localization of the  $N(A)$  electrons to the basin of atom  $A$ . The magnitude of  $F(A,A)$  is termed the *localization index*,  $\lambda(A)$ , and in general,  $\lambda(A) < N(A)$ , emphasizing that  $N(A)$  denotes an average population, the result of many electrons exchanging with the electrons in  $A$ . The total correlation shared between two basins, the quantity  $F(A,B)$ , is a measure of the number of electrons of either spin, referenced to atom  $A$ , that are delocalized onto atom  $B$  with a corresponding definition of  $F(B,A)$ . One has  $F(B,A) = F(A,B)$ , and the sum,  $|F(A,B) + F(B,A)| = \delta(A,B)$ , termed the *delocalization index*, is a measure of the number of electrons shared or exchanged between atoms  $A$  and  $B$ . Because the Fermi correlation counts all of the electrons, the localization and delocalization indices sum to  $N$ , and they provide a quantitative measure of how the  $N$  electrons in a molecule are localized within the individual atomic basins and delocalized between them. Like the Lewis model, the indices provide a bookkeeping of the electrons, but unlike the Lewis model, the tabulation is applicable to all systems at any level of theory. A corresponding relation holds for each atomic population  $N(A)$  where one has  $N(A) = \lambda(A) + \sum_{B \neq A} \delta(A,B)/2$ . This expression determines how the electron population of atom  $A$  is delocalized over the remaining atoms in the molecule.<sup>12</sup>

At the Hartree–Fock level, the delocalization index equals unity for a single pair of electrons that is equally shared between two identical atoms  $A$  and  $A'$ . Thus, the Hartree–Fock description of  $H_2$  yields  $\lambda(H) = \lambda(H') = 1/2$  and  $\delta(H,H') = 1.00$ .

The electron pairing predicted by the Hartree–Fock model of the pair density is found to be remarkably successful in recovering the Lewis model. For example, the Lewis model for  $N_2$  requires that  $\delta(N,N') = 3.00$  for three shared electron pairs and  $\lambda(N) = \lambda(N') = 5.50$ , the latter being a result of a contribution of one-half from each shared pair, two from the  $1s$  pair, and two from the nonbonded pair of electrons that is assumed to be localized on each atom. The Hartree–Fock results are  $\delta(N,N') = 3.04$  and  $\lambda(N) = 5.48$ , indicating that the nonbonded density is delocalized to a slight degree. The delocalization values for the C–C atoms in ethane and ethylene at the Hartree–Fock level are 0.99 and 1.89, respectively. The delocalization indices for such homopolar interactions decrease with the addition of Coulomb correlation, as it disrupts the pairing of electrons between the atoms. Thus, with the addition of Coulomb correlation, the value of  $\delta(H,H')$  decreases to 0.85 and  $\delta(N,N')$  to 2.2, while the values for  $\delta(C,C')$  decrease to 0.83 for ethane and to 1.42 for ethylene.<sup>12</sup> The values we report here are obtained at the Hartree–Fock level, and they will represent upper bounds to the number of Lewis electron pairs shared between equivalent atoms.

One can argue that comparisons of the Lewis model with the pairing of electrons determined by theory should be restricted to the single-determinant (Hartree–Fock) model of the wave function. It is Fermi correlation, and only Fermi correlation, that determines the spatial pairing of electrons, and this is the sole source of electron correlation at the Hartree–Fock level. In a real sense, the Hartree–Fock model retrieves the Lewis model from any, more general description of a molecular system.

The Lewis model is evident in the charge concentrations (CCs) displayed by the Laplacian of the electron density in the valence shell of charge concentration (VSCC).<sup>3,13</sup> The density is concentrated in regions where the Laplacian is negative, and thus the CCs are local maxima in the function  $L(r) = -\nabla^2\rho(r)$ . These CCs have been shown to yield a faithful mapping of the localized electron domains that are assumed to be present in the valence shell of a central atom in the VSEPR model of molecular geometry.<sup>13,14</sup> There is agreement not only in the number of CCs found in the VSCC of the central atom with the number of bonded and nonbonded electron pairs assumed in the model but also in their angular orientation and relative sizes.

The maxima in  $L(r)$  are a reflection of the spatial localization of the electrons, as shown through a study of the properties of the conditional pair density.<sup>15</sup> This density distribution shows where  $\alpha,\beta$  pairs of electrons are most likely to be found for a given position of a reference pair. The conditional pair density exhibits a very important property: *when the Fermi hole for the reference electron pair is maximally localized to a given region of space, the conditional pair density reduces to the electron density outside of the region of localization*. Under this condition, the Laplacian of the conditional pair density reduces to the Laplacian of the electron density, and the CCs of  $L(r)$  thus coincide with the local charge concentrations defined through the conditional pair density. The latter CCs indicate the positions where the density of the remaining electron pairs is most likely to be found for a fixed position of the reference pair. Thus, the CCs displayed in  $L(r)$  signify the regions of partial pair condensation, regions with greater than average

(10) Bader, R. F. W.; Stephens, M. E. *J. Am. Chem. Soc.* **1975**, *97*, 7391.

(11) Bader, R. F. W.; Johnson, S.; Tang, T.-H.; Popelier, P. L. A. *J. Phys. Chem.* **1996**, *100*, 15398.

(12) Fradera, X.; Austen, M. A.; Bader, R. F. W. *J. Phys. Chem. A* **1999**, *103*, 304.

(13) Bader, R. F. W.; MacDougall, P. J.; Lau, C. D. H. *J. Am. Chem. Soc.* **1984**, *106*, 1594.

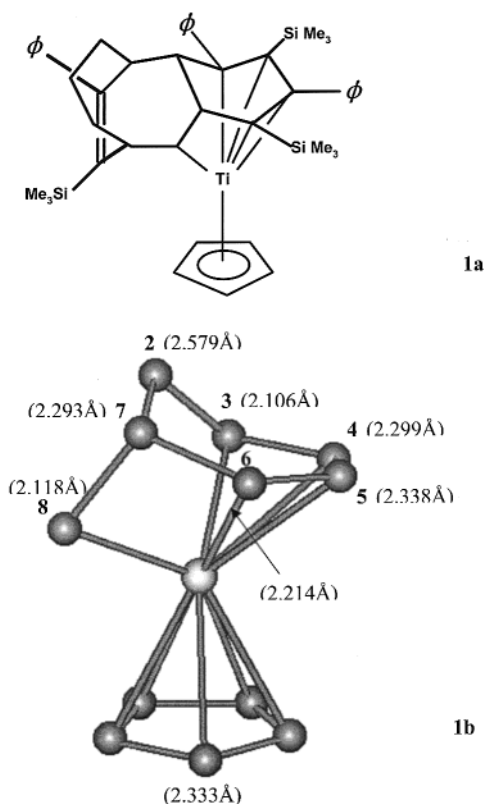
(14) Bader, R. F. W.; Gillespie, R. J.; MacDougall, P. J. *J. Am. Chem. Soc.* **1988**, *110*, 7329.

(15) Bader, R. F. W.; Heard, G. L. *J. Chem. Phys.* **1999**, *111*, 8789.

probabilities of occupation by a single pair of electrons, and  $L(r)$  provides a mapping of the essential aspects of electron pairing determined in six-dimensional space onto the real space of the density.<sup>15</sup>

### Bonding to the Titanium Atom

The complex with the short “nonbonded” Ti–C separations discussed at the meeting was synthesized by Ernst et al.<sup>1</sup> and corresponds to the structure shown as **1a**. The ligands distant to the titanium atom are omitted in the model structure **1b**, which is used by Ernst et al. and in the present paper for the purpose of discussing the bonding to the titanium atom.



The model retains the cyclopentadienyl and cyclohexadienyl fragments, the latter having an attached methylenic carbon, that constitute the carbon framework containing the atoms that are or possibly can be bonded to the titanium atom. The structure as shown is that given by Ernst et al. with their numbering system. Their structure yields “an apparent 14-electron count” by indicating the presence of bonds from Ti to atoms C3, C4, C5, and C6 of the cyclohexadiene ring (the 6-MR), to the methylene carbon, C8, and to the carbons of the cyclopentadienyl ring (the 5-MR). The lengths of the assumed Ti–C bonds are indicated in **1b**, and they are to be compared with the “remarkably short Ti–C(sp<sup>3</sup>) contacts” of Ti–C2 of 2.579 Å and Ti–C7 of 2.293 Å, the latter being less than the separations between Ti and C4, C5, or any of the carbons of the 5-MR. If these short contacts with C2 and C7 are indicative of Ti–C bonding, that is, of agostic interactions, then the complex “could provide important insight into the pathways by which C–C bonds may be selectively activated and functionalized by transition-metal centers.”<sup>1</sup>

**Computations.** Wave functions for **1b** were obtained at the restricted Hartree–Fock (RHF) and BLYP–DFT levels of theory with the experimental geometry of **1a** being used for the atoms in common with those in **1b**, followed by an energy optimization

of the carbon–hydrogen separations using GAUSSIAN 94.<sup>16</sup> The 6-31+G\* basis set was used for the carbon and hydrogen atoms, and a triple- $\zeta$  valence basis set consisting of (14s11p6d) contracted to [10s8p3d] obtained from the GAMMESS program<sup>17</sup> was used for titanium. Both sets contain diffuse functions whose presence is required for the description of possible weak interactions between carbon and titanium. The topological structure and the atomic properties were determined using PROAIM.<sup>18</sup> Delocalization indices were computed using AIM-DELOC.<sup>19</sup>

**Molecular Graph of the Titanium Complex.** The molecular graph obtained from the BLYP–DFT density is shown in Figure 1. An identical structure is obtained from the RHF density with the exception of one less bond path to the carbons of the 5-MR. Bond paths are found to reproduce the C–C and C–H interactions depicted in structure **1b**, but unlike this structure, the Ti is bonded only to the methylenic carbon, C8, and to the two terminal carbons of the diene fragment, C3 and C6, as well as to four of the carbons of the 5-MR. There are no bond paths linking Ti to the two central carbons of the diene, C4 and C5, as pictured in **1b**, and none linking Ti to the two saturated carbon atoms, C2 and C7, that exhibit the short contacts. Thus, the topology of the density does not support the presence of agostic interactions between Ti and C2 or C7. A total of 33 bond critical points, 8 ring critical points, and 1 cage critical point are found, as required to satisfy the Poincaré–Hopf relationship for the molecule, which contains 27 nuclei, and there are no missing critical points.<sup>3</sup>

**Hydrocarbon Framework Interactions.** The values of the BLYP critical point (CP) properties are given in Figure 2(a), and the RHF delocalization indices for the C–C and C–H interactions are given in Figure 2(b). Electron correlation in general decreases the value of  $\rho_b$ , the density at a bond CP,<sup>20</sup> and the RHF values of  $\rho_b$  thus exceed those obtained from BLYP by 2–3% for the C–C and C–H interactions and by <1% for the Ti–C interactions. The  $\delta(C,H)$  values indicate that approximately one Lewis pair is shared between the carbon atoms and their bonded hydrogens. The  $\delta(C,C)$  values between carbons where one or both are saturated also indicate an interaction resulting from the sharing of a single pair of electrons, while the values for the C–C interactions in the dienyl fragment and in the 5-MR indicate a sharing in excess of one electron pair. In an isolated *cis*-butadiene, the delocalization index between a terminal carbon and its bonded neighbor equals 1.83, while that between the two interior carbons is slightly greater than unity, 1.07, indicating only slight delocalization of the  $\pi$  electrons across the “single” bond. In the complex, the

- (16) Frisch, M. J.; Trucks, G. W.; Schlegel, H. B.; Gill, P. M. W.; Johnson, B. G.; Robb, M. A.; Cheeseman, J. R.; Keith, T.; Petersson, G. A.; Montgomery, J. A.; Raghavachari, K.; Al-Laham, M. A.; Zakrzewski, V. G.; Ortiz, J. V.; Foresman, J. B.; Cioslowski, J.; Stefanov, B. B.; Nanayakkara, A.; Challacombe, M.; Peng, C. Y.; Ayala, P. Y.; Chen, W.; Wong, M. W.; Andres, J. L.; Replogle, E. S.; Gomperts, R.; Martin, R. L.; Fox, D. J.; Binkley, J. S.; Defrees, D. J.; Baker, J.; Stewart, J. P.; Head-Gordon, M.; Gonzalez, C.; Pople, J. A. *Gaussian 94*, revision B.3; Gaussian, Inc.: Pittsburgh, PA, 1995.
- (17) Schmidt, M. W.; Baldrige, K. K.; Boatz, J. A.; Elbert, S. T.; Gordon, M. S.; Jensen, J. H.; Koseki, S.; Matsunaga, N.; Nguyen, K. A.; Su, S. J.; Windus, T. L.; Dupuis, M.; Montgomery, J. A. *J. Comput. Chem.* **1993**, *14*, 1347.
- (18) Biegler-König, F. W.; Bader, R. F. W.; Tang, T.-H. *J. Comput. Chem.* **1982**, *13*, 317.
- (19) Matta, C. F. *AIMDELOC01 (LNUX101/QCPE0802): Program to Calculate AIM Localization and Delocalization Indices*; Quantum Chemistry Program Exchange, Chemistry Department, Indiana University: Bloomington, IN, 2001 (<http://qcpe.chem.indiana.edu/>).
- (20) Gatti, C.; MacDougall, P. J.; Bader, R. F. W. *J. Chem. Phys.* **1988**, *88*, 3792.



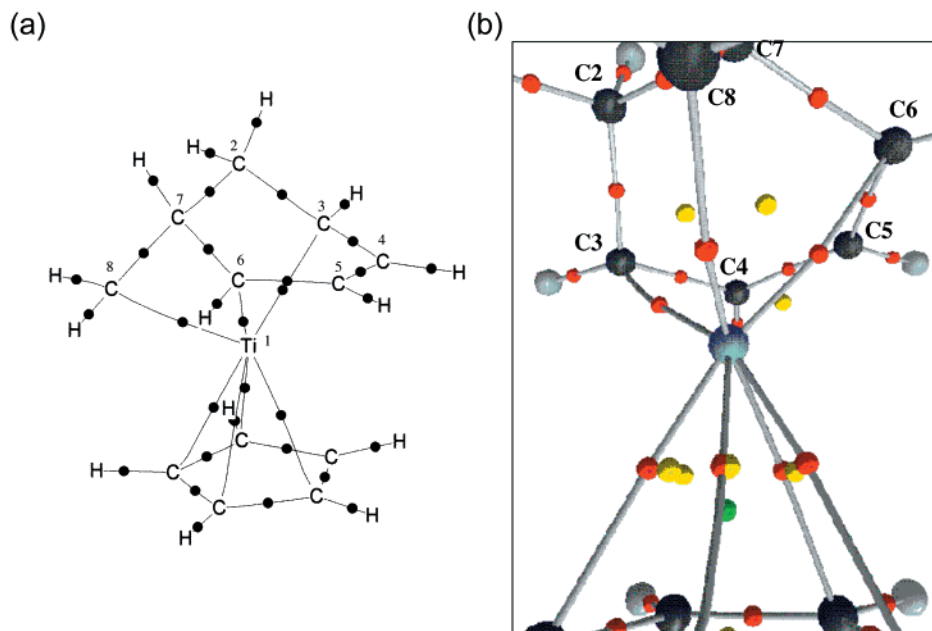


**Figure 1.** (a) Projection of the molecular graph for **1b** determined by the topology of the BLYP electron density. A bond critical point (CP) is denoted by a dot. It denotes the intersection of the bond path with the interatomic surface. Note the curvature of the Ti–C bond paths at their termini with the carbons of the 5-MR. (b) Positions of the ring CPs are denoted by yellow dots, except for the 5-MR, which is not included in the diagram. The Ti–C bond and associated ring CPs of the 5-MR are linked by an almost constant ring of density signifying the presence of a bonded cone of density enclosing a cage critical point denoted by a green dot. The bond CP of the Ti–C bond path in the central foreground of the figure is nearly superimposed on a neighboring ring CP, and the bond path is on the verge of annihilation. In the text, the carbons of the 5-MR are labeled C1' to C5' with C1' in the foreground of (a) and counting anticlockwise.

bonding of the terminal atoms, C3 and C6, to Ti reduces the delocalization indices  $\delta(\text{C3,C4})$  and  $\delta(\text{C5,C6})$  from 1.83 in the free diene to 1.2 and 1.3, respectively, a result of C3 and C6 sharing density with the Ti. The two interior atoms, C4 and C5, are not bonded to the Ti, as proposed by Ernst et al.;<sup>1</sup> consequently,  $\delta(\text{C4,C5})$  increases from 1.07 to 1.5, and they retain their unsaturated nature. The change in the delocalization indices for the dienyl carbons from the values found in the free diene is suggestive of a Diels–Alder-type addition of the Ti, with the metal bonding restricted to the two terminal atoms and  $\pi$  density being transferred between the two central carbons.

The indices for nonneighboring atoms indicate that the sharing of electrons between such atoms is negligibly small when one or both of the atoms are saturated carbons, but they are equally indicative of significant delocalization of electrons over the conjugated atoms of the 6- and 5-MRs.

The values of the bond CP properties are typical of nonpolar shared C–C and C–H interactions:  $\rho_b$  ranging from 0.21 to 0.28 au for the C–C interactions in the 6-MR and including C8, the values increasing in parallel with the increase in  $\delta(\text{C,C})$ , the number of shared electron pairs. The largest value, 0.31 au, is found for the 5-MR. The values of  $\nabla^2\rho_b$  are all negative, the magnitude increasing with the value of  $\delta(\text{C,C})$ . The local expression for the virial theorem equates  $(1/4)\nabla^2\rho_b$  to the sum of  $2G_b$ , the kinetic energy density, and  $V_b$ , the potential energy density. Since  $G_b > 0$  and  $V_b < 0$ , the finding that  $\nabla^2\rho_b < 0$  demonstrates that the interactions are stabilized by the decrease in the potential energy that results from the contraction of the electron density toward the bond path and to its accumulation in the binding region, both effects increasing with the value of  $\delta(\text{C,C})$ . The energy density,  $H_b$ ,<sup>21</sup> is given by the sum  $G_b + V_b$ , and its magnitude parallels the value of  $\rho_b$  for the 6-MR and 5-MR rings. The largest magnitudes of  $\nabla^2\rho_b$  and  $H_b$  and of the potential energy density  $V_b$  are found for the delocalized charge distribution of the 5-MR, a system associated

with “resonance” stabilization. These same atoms are more stable than C2, the least stable carbon atom of the 6-MR, by an amount in excess of 120 kcal/mol. The bond paths and their properties, together with the electron delocalization data, demonstrate that theory is able to both recover and make quantitative the classical descriptors of bonding for the hydrocarbon framework. The same theory is next applied to the interactions with the Ti atom where the classical models can fail.

**Titanium–Carbon Interactions.** Data summarizing the Ti–C interactions are given in Figure 3. We first comment on the bonding between Ti and the carbons of the 5-MR. The bond paths are characterized by relatively small values of  $\rho_b$ ,  $\sim 0.05$  au, values considerably less than those for the C–C and C–H interactions. The Ti–C bond paths to bonded pairs of carbon atoms (C1'–C2', C4'–C5', and C5'–C1') form 3-MRs, and a ring CP is present in the face of each ring. Another ring is formed by the closed loop of interactions of Ti–C2'–C3'–C4'–Ti. Each of these rings possesses a CP in the associated ring surface where the electron density attains its minimum value, a value denoted by  $\rho_r$ . There is also a ring critical point in the face of the 5-MR, and together, these ring faces define a cage enclosing a cage critical point where the density attains a minimum value (Figure 1(a),(b)). What is special about the rings formed with the Ti is that the values of  $\rho_r$  are only slightly less than the values of  $\rho_b$  for the Ti–C bond paths, the lowest values for the density in the perimeter of each ring. In addition, all of the bond and ring CPs are approximately equidistant from the Ti atom,  $2.07 \pm 0.02$  Å, and as a result, a ring of nearly constant density,  $\rho = 0.050 \pm 0.003$  au, encircles the bonded cage, as indicated in Figure 1(b). Thus, the bonding of the Ti to the carbons of the 5-MR is not well represented in terms of individual atomic interactions but rather by a *bonded cone* of density, with the individual bond paths having values for the density only in slight excess of the density in the face of each

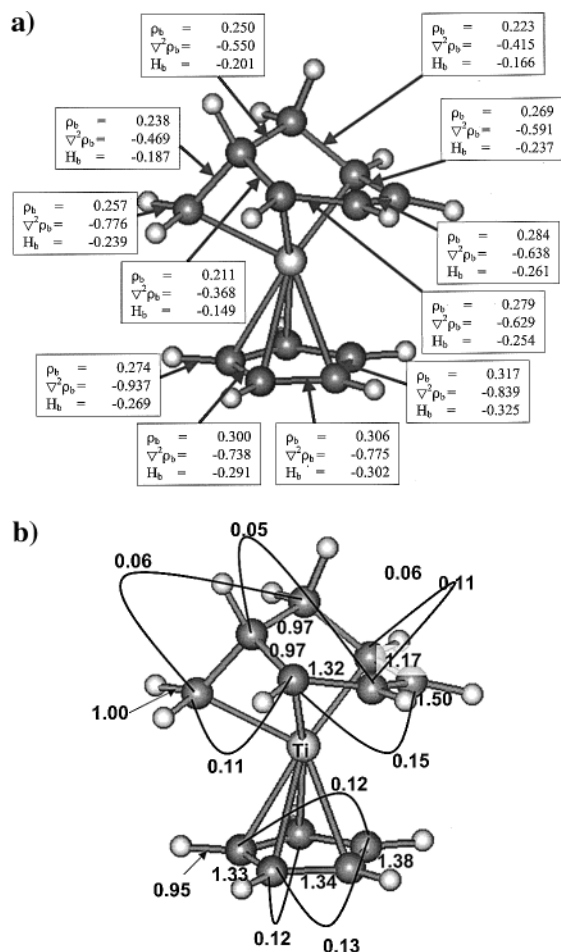


**Figure 2.** (a) Depiction of the molecular graph wherein the nuclei are denoted by spheres and the bond paths by lines to display the BLYP values of properties at the C–C and two typical C–H bond CPs of the hydrocarbon framework: the electron density,  $\rho_b$ , the Laplacian of the density,  $\nabla^2\rho_b$ , and the energy density,  $H_b$ . The magnitudes of all three bond descriptors increase with the assumed classical bond order, the values for the central bond of the diene fragment, C4–C5, exceeding those for the two terminal bonds. (b) Hartree–Fock values of the delocalization index  $\delta(C,C')$  for neighboring (bonded) and next nearest (NN) neighboring carbon atoms, the NN pair of atoms being linked by a curved line. Note that there are significant NN neighbor delocalizations only between pairs of unsaturated atoms with the exception of the value of 0.11 between the methylenic carbon, C8, and C6 of the diene fragment.

ring that links one Ti–C interaction with the neighboring one. This situation is pictured in Figure 4, which shows the cone-shaped density envelope for a value equal to the average density of the bond and ring CPs lying in the bonded cone. Note that the cone extends out to all of the atoms of the cyclopentadienyl ring since the ring CPs, including that of the 4-MR, are all approximately equidistant from the axis of the ring of carbon atoms. Clearly, the interaction of a metal atom with the carbons of a cyclopentadienyl ring is best viewed as involving the delocalized density of the entire ring perimeter, a picture that is conceptually similar to that used to denote a metal–ring interaction in a conventional structure diagram, **1a**. The topological description provides a real space representation of Moffitt’s view of the bonding in cyclopentadienyl molecules in terms of “cup-shaped lobes” formed from d orbitals on the metal overlapping with the ring of  $\pi$  orbitals on the 5-MRs.<sup>22</sup>

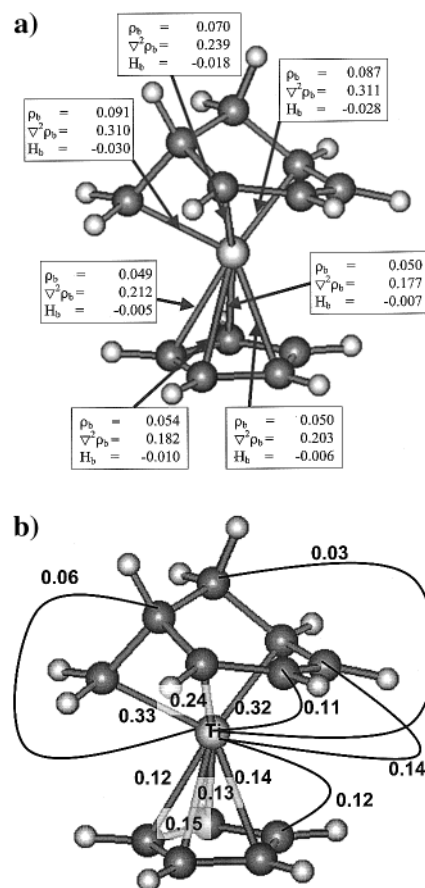


**Figure 3.** (a) BLYP values of the Ti–C bond critical point data. Note the parallel increase in the magnitude of the energy density  $H_b$  with  $\rho_b$ . (b) Hartree–Fock delocalization indices for the Ti–C bonded interactions and for the delocalization between Ti and the carbons to which it is not bonded. The values of  $\delta(\text{Ti–C})$  for the “close contact” carbons, C2 and C7, are no larger than those found for the delocalizations between next nearest carbon atoms where one or both are saturated (Figure 2(b)). The electron density is nearly uniformly delocalized between Ti and the carbons of the 5-MR that are linked by the bonded cone of density.

The result is an enhanced binding over what one would anticipate on the basis of the individual  $\rho_b$  values. This view of the bonding to the 5-MR is consistent with the observation that the barrier to free rotation of a cyclopentadienyl ring in metal complexes is quite low. Moffitt shows that a single electron pair is involved in the bonding of a metal atom to a Cp ring and the interaction is formally electron deficient. Thus, it is not surprising that the bonding topology found in Ti–Cp bonds is the same as that found for the boranes and carboranes.<sup>23</sup> The stability of these electron-deficient molecules has been shown to be a consequence of the delocalization of the density over the surfaces of 3- and 4-MRs of bonded boron and or carbon atoms, a picture that is in agreement with the description of these systems as globally delocalized by King and Rouvray.<sup>24</sup> Since the density is almost flat along a line linking a ring CP to the two neighboring Ti–C bond CPs, the associated curvatures of the density at all three CPs approach zero and the Ti–C bond CPs exhibit large ellipticities. That is, the negative curvature of  $\rho$  at a bond CP tangent to the ring of CPs is much smaller in magnitude than the one normal to it and to the bond path. Only a small amount of vibrational energy is required to

(21) Cremer, D.; Kraka, E. *Angew. Chem.* **1984**, *23*, 627.

(22) Moffitt, W. *J. Am. Chem. Soc.* **1954**, *76*, 3386.

(23) Bader, R. F. W.; Legare, D. A. *Can. J. Chem.* **1992**, *70*, 657.

(24) King, R. B.; Rouvray, D. H. *J. Am. Chem. Soc.* **1977**, *99*, 7834.

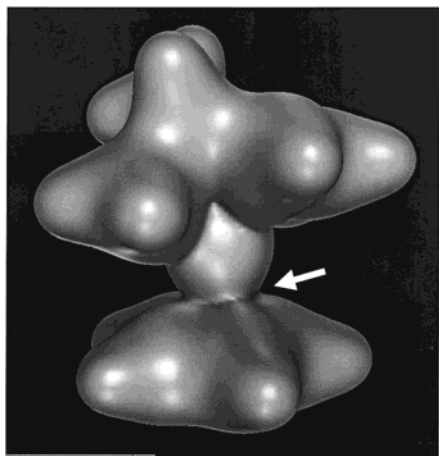


**Figure 4.** Display of an envelope of the electron density for a value equal to the average of the bond and ring CP values that form the ring of density in the surface of the bonded cone. These CPs lie in the interatomic surfaces that separate the Ti atom from the carbon atoms of the 5-MR ring, and the ring of density they define, denoted by an arrow in the figure, lies at the union of the Ti atom density with that of the 5-MR. The ring represents the minimum value in the cone of density that links the Ti nucleus to the carbon nuclei of the 5-MR (Figure 1(a)).

perturb the form of the density in the region where its curvatures are vanishingly small.<sup>3,25</sup> In the present case, the perturbation causes a ring CP to coalesce with one of the neighboring bond CPs, resulting in the formation of a singularity in the density, a CP where both the first and second derivatives of the density vanish along the line of approach of the two CPs. Such a CP is unstable, and any further nuclear motion results in its annihilation and in the rupture of the associated Ti–C bond path. It is clear from Figure 1(b) that the central Ti–C bond path of the cage is on the verge of annihilation, as its bond CP and the neighboring ring CP are nearly superimposed, being separated by only 0.054 au. In turn, their densities differ by only  $1 \times 10^{-6}$  au, and their respective curvatures are  $-0.001$  and  $+0.002$  au. It is this bond path that is missing in the Hartree–Fock density. The density in the face of the 4-MR in the bonded cone is also flat, and a motion of the nuclei can result in the creation of a new singularity that bifurcates into a new bond and a new ring CP. The magnitudes of the associated curvatures of the bond and ring CPs are 0.008 au, compared to a value of 0.26 au for the curvature along the Ti–C bond path. These two structural changes are not independent, and low-energy ring-puckering motions will constantly cause the annihilation and creation of Ti–C bond paths, leaving the bonded cone of density intact at all times. In  $\text{Ti}(\text{C}_5\text{H}_5)^+$ , Ti is symmetrically placed with respect to the carbons of the 5-MR and is linked by bond paths with large ellipticities to all five carbon atoms. The Ti–C bond and the 3-MR ring CPs yield a ring of density that varies by only 0.0006 au between its maximum and minimum values. The bond CPs exhibit large ellipticities, with a curvature of small magnitude tangent to the ring of CPs. The curvatures of the density at the bond and ring CPs alternate between  $-0.006$  au at the bond CPs and  $+0.006$  au at the ring CPs, the topological requirements for the continuous making and breaking of Ti–C bond paths by low-amplitude ring-puckering motions. Large ellipticities are also found for the agostic interactions of Ti with H in  $\text{C}_2\text{H}_5\text{TiCl}_3(\text{dmpe})$  and  $\text{C}_3\text{H}_7\text{TiCl}_2^+$ ,<sup>6,7</sup> indicative of their topological instability. The formation of the agostic bond results in the formation of a ring structure, and it is broken by the

coalescence of the bond CP with the associated ring CP that occurs with a rotation about a C–C axis.

While the three bonded interactions of the Ti with carbons of the remaining framework exhibit larger values for  $\rho_b$  than those found for the 5-MR, they all exhibit similar characteristics:  $\rho_b < 0.1$  au,  $\nabla^2\rho_b > 0$ , and  $H_b < 0$ . The CP data are similar to those obtained in theoretical calculations of Ti–C interactions in  $\text{CH}_3\text{TiCl}_2^+$  and  $\text{Ti}(\text{CH}_3)_2\text{Cl}_2$ .<sup>6,26</sup> The Ti–C bond lengths in these molecules, from 1.97 to 2.03 Å, respectively, are shorter than those in the present molecule where the shortest distance is 2.12 Å and the  $\rho_b$  values of  $\sim 0.12$  au are somewhat larger. The experimental value of  $\rho_b$  (0.082 au) determined for Ti–C in  $\text{TiCl}_3(\text{dmpe})$  with the Ti–C separation equal to 2.15 Å<sup>7</sup> is in good agreement with the value reported here for Ti–C8 with  $\rho_b = 0.091$  au for a bond length of 2.12 Å. The longer bond lengths and smaller  $\rho_b$  values found for the molecules where the Ti is bonded to a large complex organic ligand indicate weaker Ti–C interactions than are predicted for bonds to the carbons of a methyl group.

The longer Ti–C bond lengths found in **1b** compared to those of a Ti bonded to a carbon of a methyl group result in values of  $\nabla^2\rho_b$  that are approximately 10 times larger, ranging from 0.2 to 0.3 au. Small values of  $\rho_b$  and positive values of  $\nabla^2\rho_b$  for bonds between main group atoms are usually found for closed-shell interactions, which include ionic interactions between ions that approach closed-shell electronic structures. In these cases, the kinetic energy density at the bond CP so outweighs the potential energy density that the total energy density  $H_b$ , and  $\nabla^2\rho_b$ , are both positive. In the case of interactions between transition metal atoms or between a transition metal atom and a ligand, however,  $H_b$  appears to be invariably negative. Thus, bonding to a transition metal defines a new set of bond CP characteristics that represent a mix of the closed-shell and shared parameters, with  $\rho_b$  being small and  $\nabla^2\rho_b > 0$ , as found for a closed-shell interaction, but with  $H_b < 0$ , as found for a shared interaction.<sup>27,28</sup> The magnitude of  $H_b$  parallels the increase in the values of  $\rho_b$  and  $\nabla^2\rho_b$  (Figure 3). The positive values of  $\nabla^2\rho_b$  are discussed further below.

There is considerable charge transfer from Ti to the ligands, as indicated by the atomic charges displayed in Figure 5(a), with Ti losing approximately three electronic charges. The charge on the  $\text{C}_5\text{H}_5$  group is  $-0.8 e$ . Hydrogen transfers electronic charge to an unsaturated carbon, and the net charge on the cyclopentadienyl carbons is  $-1.1 e$ . The increasing amount of electronic charge transferred to each of the three other carbons bonded to Ti, C3, C6, and C8 parallels the increase in their associated  $\rho_b$  value. The other carbons bearing significant negative charges are the remaining members of the dienyl group, C4 and C5, which also withdraw electronic charge from their bonded hydrogens. The electronegativity of a carbon atom decreases with decreasing s character, and carbons in saturated hydrocarbons bear small positive charges. In **1b**, the two saturated carbons, C2 and C7, bear small negative charges as a result of charge transfer from Ti.

Figure 5(b) gives the energies of both sets of carbon atoms relative to those of the least stable atom in each set. In each case, this is a carbon not bonded to Ti. The most stable atoms are those bonded to the Ti, and the degree of stabilization increases in parallel with the value of  $\rho_b$  and with the magnitude of the negative charge on carbon within each set.

(26) Bader, R. F. W.; Gillespie, R. J.; Martín, F. J. *Chem. Phys. Lett.* **1998**, *290*, 488.

(27) Macchi, P.; Proserpio, D. M.; Sironi, A. *J. Am. Chem. Soc.* **1998**, *120*, 13429.

(28) Frenking, G.; Pidun, U. *J. Chem. Soc., Dalton Trans.* **1997**, 1653.

(25) Bader, R. F. W.; Laidig, K. E. *J. Mol. Struct.* **1992**, *261*, 1.



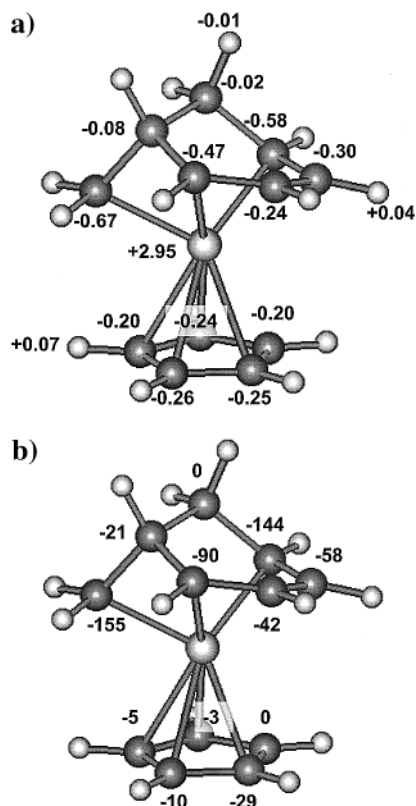


**Figure 5.** (a) BLYP atomic charges for **1b**. (b) BLYP energies in kcal/mol of the carbon atoms in the cyclohexadienyl fragment relative to the energy of C2, and energies of the carbons in the 5-MR relative to the energy of the carbon not bonded to Ti. Hartree–Fock values are nearly identical and yield the same trends. The carbons of the 5-MR are more stable than C2 by 123 kcal/mol, and the most stable carbon atoms in each set are those that are bonded to the Ti atom.

The delocalization indices  $\delta(\text{Ti},\text{C})$  for the bonded interactions also increase along with the values of  $\rho_b$  (Figure 3(b)), but all are considerably smaller than the values of  $\delta(\text{C},\text{C})$  found for the hydrocarbon framework. The value of the delocalization index equals the number of shared Lewis pairs only for homopolar bonding. In the presence of charge transfer, as found for the Ti–C interactions, the electron pair is not equally shared but partly localized on the more electronegative atom, that is,  $\lambda(\text{C})$  increases at the expense of  $\delta(\text{Ti},\text{C})$ . Quite independent of the Lewis model,  $\delta(\text{Ti},\text{C})$  determines the extent to which electrons are exchanged between Ti and a carbon atom, and this value is greatest for the atoms bonded to Ti within each set. This value is the least for atoms C2 and C7, their values of  $\delta(\text{Ti},\text{C}) = 0.03$  and  $0.06$ , respectively, being no greater than those determining the delocalization of their electrons into the basins of carbon atoms to which they are not bonded, values of  $0.06$  or smaller. These are to be compared to values of  $\delta(\text{Ti},\text{C})$  ranging from  $0.2$  to  $0.3$ , for the carbon atoms bonded to Ti within the same set. The only saturated carbon with a significant delocalization into the basin of an atom it is not bonded to is C8 and its delocalization is into the basin of C6, both of which are bonded to Ti.

The atomic population of Ti equals 19 electrons (and hence bears a charge of  $+3e$ ) of which approximately 18 are localized within its own basin, meaning that approximately one electronic charge is delocalized into the basins of other atoms. The number of localized electrons ( $\lambda(\text{Ti}) = 17.9$  for both RHF and BLYP) corresponds to a nearly complete localization of the density of the inner quantum shells (2,8,8), and the net charge of  $+3$

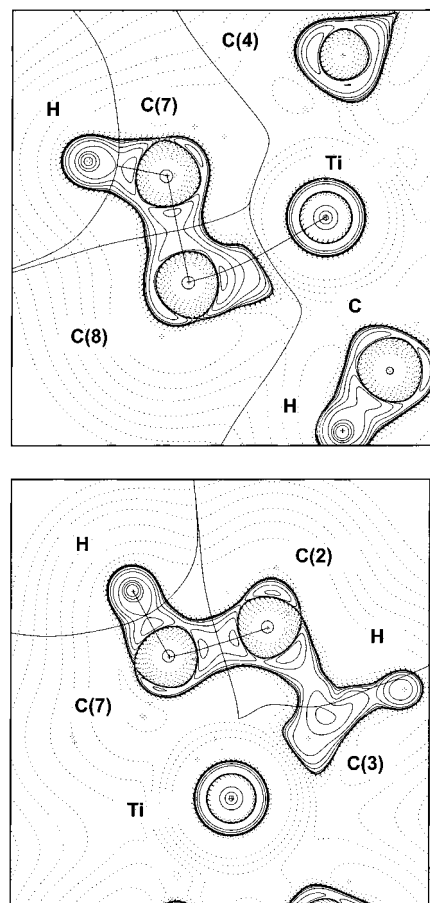


**Figure 6.** Contour maps of the Laplacian of the electron density with solid contours denoting regions of charge concentration where  $\nabla^2\rho < 0$ . Bond paths in the plane are indicated as are projections of interatomic surfaces onto the plane. (a) A plane containing the Ti, C8, and C7 nuclei, slightly above the nucleus of a carbon of the 5-MR. C8 exhibits four CCs characteristic of a saturated carbon: two bonded CCs directed at hydrogens above and below this plane and evident in Figure 7, a bonded CC to C7, and a very pronounced bonded CC directed at the Ti atom. (b) A plane containing the Ti, C7, and C2 nuclei and showing the pronounced bonded CC from C3 directed at the Ti atom. Both C7 and C2 exhibit four bonded CCs. C2, for example, possesses a bonded CC to C7, two bonded CCs to out-of-plane hydrogens, and another bonded CC to C3. Neither C2 nor C7 exhibits a bonded CC directed at the Ti atom. Contours in the nonbonded regions of the carbon atoms denote (3, -1) CPs that link the bonded charge concentrations.

corresponds to the loss of all but one of its valence electrons. Of the one electronic charge that is delocalized,  $0.7$  is shared with the carbons to which it is bonded,  $0.4$  to C8, C3, and C4, and  $0.3$  with the carbons of the 5-MR. Another  $0.1$  is shared with the unsaturated atoms, C4 and C5, and the remaining  $0.2$  is delocalized over all of the other atoms in the molecule.

**Laplacian and Bonding to Titanium.** A carbon atom exhibits two quantum shells in  $L(r) = -\nabla^2\rho$ , as shown in the contour maps of  $L(r)$  in Figure 6. In accordance with the Lewis and VSEPR models, the VSCC of each saturated carbon atom exhibits four bonded charge concentrations in a tetrahedral arrangement and the VSCC of each of the unsaturated carbons exhibits three such concentrations in a trigonal arrangement. These local maxima in the VSCC of an atom are located and identified, along with the other possible CPs in  $L(r)$ , using PROAIM.<sup>18</sup> Each carbon bonded to Ti, that is, linked to it by a bond path, has a CC directed at the Ti core. Spatial displays of the geometric patterns of CCs are illustrated in Figure 6 and by the zero-envelope of the Laplacian of the density in Figure

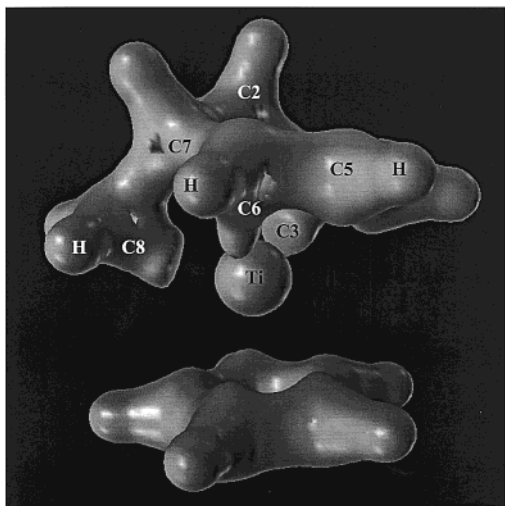


**Figure 7.** Zero-envelope map of the Laplacian of the electron density that encloses the regions of charge concentration. The extension protruding from C8 is the bonded CC directed at the Ti core. Similar extensions are found protruding from C6 and C3. The secondary charge concentrations directed at the Ti from the carbons of the 5-MR are also evident.

7. The zero-envelope defines the outer boundary of the VSCC on the carbons, hydrogens, and the outer core of Ti. Included in the group of saturated carbons with four bonded CCs are C3 and C6, the terminal carbons of the dienyl system that are bonded to Ti. The inner atoms of the dienyl group, C4 and C5, exhibit only three CCs as found for a  $sp^2$  carbon. The bonded CC on each of the atoms (C3, C6, and C8) that is directed at the Ti core is clearly evident in Figures 6 and 7. There is no CC on C2 or C7 that is directed at Ti. There is no suggestion of the formation of a fifth CC on C2 or C7 directed at Ti either. The carbons of aromatic ring systems such as benzene and cyclopentadienyl display a set of secondary CCs on each carbon, on each side of the ring system.<sup>29</sup> These are evident in Figure 6 and in the zero-envelope (Figure 7) where they appear directed at the Ti atom.

The Laplacian of a transition metal atom does not possess a valence shell charge concentration, whether free or bound. This is not an artifact of the shell structure defined by the Laplacian, but is determined by the conditional pair density.<sup>15</sup> The Laplacian of the conditional pair density, which is homeomorphic with the Laplacian of the electron density for a localized reference pair, demonstrates that there is no separate localization of electrons beyond the shell of charge concentration found for the  $(n - 1)$  shell of the core for a transition metal atom in row  $n$  of the periodic table. This is evident in the contour plots of the Laplacian of the density given in Figure 6. In addition to the spikelike charge concentration at the position of the Ti nucleus, there are two essentially spherical shells of charge concentration, indicating the presence of three quantum shells for the Ti atom, the zero-envelope surface of the third shell appearing in Figure 7. Because of the lack of a VSCC, the interatomic surfaces of the bonded neighbors all border on the outer shell of charge depletion of a transition metal atom, a feature that accounts for the ubiquitous appearance of positive  $\nabla^2\rho_b$  values for bonding to a transition metal atom.

The Laplacian of a transition metal differs from that of a main group atom in a second fundamental way: no bonded charge concentrations are found within its outer shell of charge

concentration. Instead, the maxima associated with the ligands that are present are opposed to, rather than adjacent to, the position of the ligands and are labeled as ligand-opposed CCs (LOCCs). This important topological feature of  $L(r)$  is found both theoretically<sup>11,30,31</sup> and experimentally.<sup>32–36</sup> It is important to note that the LOCCs are formed from the remaining  $n$  s electrons and  $(n - 1)$  d electrons on the transition metal atom whose density is concentrated in the same shell of charge concentration as are the  $(n - 1)$  s and p electrons of the core.<sup>26</sup> In the present case, with only one valence electron remaining on Ti and that is strongly delocalized onto the ligands, the local maxima in  $L(r)$  representing the LOCCs are nearly indistinguishable from the neighboring minima and the outer shell of Ti appears spherical (Figure 7). Ti does display LOCCs when the charge on Ti is  $\leq +2$ , corresponding to the presence of two or more valence electrons.<sup>26</sup> Thus, CCs opposed to the carbons of the 5-MR are displayed within the outer core of Ti in  $Ti(C_5H_5)^+$  where the charge on Ti is approximately  $+2 e$ .

While the Lewis model of bonding is recovered in the pattern of bonded and nonbonded CCs of  $L(r)$  for main group atoms, this is clearly not the case for the topology of  $L(r)$  displayed by a bound transition metal atom, and the classical models of bonding must be abandoned. As illustrated in this paper, one can use model-independent properties determined by the electron density and the pair density that have been shown to successfully account for the bonding in main group elements to aid in the carryover of the traditional models to obtain an understanding of transition metal bonding.

## Conclusions

Theory gives physical expression to the chemical concepts of bonding, structure, and electron delocalization, and it recovers the classical descriptors of bonding within the hydrocarbon framework of the complex. The use of theory in the description of the bonding between this framework and the Ti atom is thus justified. The electron density and the Laplacian of the density and the conditional pair density demonstrate that Ti is bonded to the methylenic carbon C8, to the terminal atoms C3 and C6 of the dienyl fragment in the 6-MR, and to the carbons of the 5-MR in a fluxional manner. No bonded interactions are present between Ti and the inner atoms C4 and C5 of the dienyl fragment, and the interaction of Ti with the diene fragment corresponds to a Diels–Alder addition. There are no bonded interactions of Ti with atoms C2 and C7 that exhibit short “nonbonded” Ti–C separations, and they retain the characteristics of tetrahedrally bonded saturated carbon atoms. The atomic charges and energies also clearly differentiate between the carbons that are bonded to Ti and those that are not.

The electron density distribution does not give any indication of incipient structural change resulting from the formation of a singularity in  $\rho$  in the region between Ti and C2 or C7 or between Ti and C4 or C5. Instead, the density exhibits steep troughs between the basins of these pairs of atoms with correspondingly large curvatures along the line linking their

(29) Bader, R. F. W.; Chang, C. *J. Phys. Chem.* **1989**, *93*, 6.

(30) Gillespie, R. J.; Bytheway, I.; Tang, T.-H.; Bader, R. F. W. *Inorg. Chem.* **1996**, *35*, 3954.

(31) Gillespie, R. J.; Bayles, D.; Platts, J.; Heard, G. L.; Bader, R. F. W. *J. Phys. Chem. A* **1998**, *102*, 3407.

(32) Smith, G. T.; Mallinson, P. R.; Frampton, C. S.; Farrugia, L. J.; Peacock, R. D.; Howard, J. A. K. *J. Am. Chem. Soc.* **1997**, *119*, 5028.

(33) Wang, C. C.; Wang, Y.; Liu, H.-J.; Lin, K.-J.; Chou, L.-K.; Chan, K.-S. *J. Phys. Chem. A* **1997**, *101*, 8887.

(34) Hwang, T. S.; Wang, Y. *J. Phys. Chem. A* **1998**, *102*, 3726.

(35) Lee, C.-R.; Wang, C.-C.; Chen, K. C.; Lee, G.-H.; Wang, Y. *J. Phys. Chem. A* **1999**, *103*, 156.

(36) Spackman, M. A. *R. Soc. Chem. Annu. Rep., Sect. C* **1998**, *94*, 183.



nuclei. For example,  $\rho$  attains a minimum value of 0.047 au, 2.0 au from Ti and 2.3 au from C7 on the line linking their nuclei. Diagonalization of the Hessian of the density at this point yields one negative and two positive curvatures, and the largest of the two positive curvatures, 0.268 au, is directed along the Ti–C7 axis to within 1.5°. The value of this curvature is hundreds of times larger than those recorded above as portending structural changes of the Ti with the carbons of the 5-MR, and its value precludes any possibility of structural change for motions confined to the bonded wells on the potential energy surface. A BLYP optimization of the geometry in which only the dihedral angles were fixed at the experimental values resulted in both of the “close contacts” to C2 and C7 increasing by 0.04 Å. The molecule is not on the verge of forming bond paths from Ti to either of these atoms. A bond path, again with a significant ellipticity, denoting an agostic interaction of Ti with the terminal saturated carbon atom is found in  $C_3H_7TiCl_2^+$  at HF, BLYP, and MP2 levels of theory,<sup>6</sup> indicating that such an interaction is possible and is identified by theory when present.

Ernst et al.<sup>1</sup> cite “remarkably low”  $^{13}C$  coupling constants for pairs of atoms involving C2 or C7 as evidence of an agostic interaction between Ti and these saturated carbons. The coupling constant for C2–C7 itself is normal, and only those couplings between pairs of atoms that involve one atom linked to the Ti by a bond path exhibit low values. The values increase in the order C6–C7, C3–C2, and C8–C7, an order that parallels the decrease in bond length, including that for C2–C7, which possesses the shortest bond length and largest coupling constant. The principal contribution to a coupling constant is from the Fermi contact term resulting from the electron spin density induced at one nucleus by the nuclear moment of the other. Such spin information is transmitted by the delocalization of the spin density as described by the individual spin contributions to the delocalization index.<sup>37</sup> Only those coupling constants that involve an atom that has significant delocalization onto the Ti atom, that is, those linked to Ti by a bond path, have “low” values.

Ernst et al.<sup>1</sup> employ natural atomic and bond orbital analyses to describe the changes that result from the addition of

$Ti(C_5H_5)^+$  to a 5-methylene-1,3-cyclohexadiene anion. The changes are described in terms of orbital overlaps, the occupancy of C–H and C–C bond orbitals, and overlap-weighted bond orders. Without criticizing the natural orbital analysis in particular, it is a feature of the orbital model that any chosen representation is but one of many obtainable by a unitary transformation of some initial set, all of which leave the physics and chemistry of the system unchanged. Relating an observed effect to the properties of individual orbitals leaves open the possibility of compensating changes occurring in other members of the set. The use of orbital contributions to interpret magnetic properties, for example, is without physical meaning, as the orbital contributions to the total induced current do not individually satisfy the condition of being divergence free, and they thus correspond to the local creation or destruction of electronic charge. Unlike atoms defined as quantum open systems, orbitals or orbital-derived quantities, however they are defined, are not confined to the atoms or bonds they are associated with when used to define a population or a bond order.

Consider, for example, the “significant overlap weighted NAO bond order” of 0.168 they find for Ti–C7.<sup>1</sup> The delocalization of electrons, a property underlying the notion of bond order, is uniquely determined by the pair density and is independent of the orbital representation used to determine it.<sup>10</sup> Indeed, all pairs of orbital products contribute to both  $\lambda(A)$  and  $\delta(A,B)$  at all levels of theory. Using the physical definition of “bond order”, one finds the delocalization of electrons between Ti and C7 to be minimal, equal to that found between next nearest neighbor saturated carbon atoms (Figure 3(b)).<sup>12</sup> There is no observable property of any system,<sup>3</sup> including one induced by an external field<sup>38–40</sup> or by the absorption of light,<sup>41</sup> whether measured directly or obtained through a combination of measured values, that cannot be predicted using the physics of an open system, the physics of an atom in a molecule.

IC0101650

(37) Bader, R. F. W.; Streitwieser, A.; Neuhaus, A. L. K. E.; Speers, P. J. *Am. Chem. Soc.* **1996**, *118*, 4959.

(38) Bader, R. F. W.; Gough, K. M.; Laidig, K. E.; Keith, T. A. *Mol. Phys.* **1992**, *75*, 1167.

(39) Bader, R. F. W.; Keith, T. A. *J. Chem. Phys.* **1993**, *99*, 3683.

(40) Keith, T. A.; Bader, R. F. W. *Can. J. Chem.* **1996**, *74*, 185.

(41) Bader, R. F. W.; Bayles, D.; Heard, G. L. *J. Chem. Phys.* **2000**, *112*, 10095.